Seventh International Conference on
Computational Fluid Dynamics (ICCFD7),
Big Island, Hawaii, July 9-13, 2012

ICCFD7-2303

Pressure Statistics from Direct Simulation of Turbulent Boundary Layer

A.G. Gungor[1,2], J.A. Sillero[2] and J. Jiménez[2]
Corresponding author: ayse.gungor@itu.edu.tr

[1] Faculty of Aeronautics and Astronautics, Istanbul Technical University,
34469 Istanbul, Turkey.
[2]School of Aeronautics, Universidad Politécnica de Madrid, 28040 Madrid, Spain.

Abstract: The dynamics of the pressure fluctuations are analyzed using a relatively large-scale direct simulation of a turbulent boundary layer. Proper turbulent inflow conditions, key in boundary layers, are generated by an auxiliary simulation at lower resolution and Reynolds number. Special emphasis is put on the contamination of the pressure statistics due to the inflow boundary conditions. It is shown that extraneous pressure fluctuations are due to the variations in the mass-flow rate at the inflow, and a remedy is proposed.

Keywords: Direct Numerical Simulation, Turbulent Boundary Layers, Pressure Fluctuations.

1 Introduction

The behavior of the pressure in turbulent boundary layers is of special interest in engineering, because its fluctuations contribute to aerodynamic noise and flow-induced vibration. They are also important in redistributing the turbulence activity across scales, and understanding them is critical for modeling purposes. Unfortunately, they are difficult to obtain experimentally, in part because of instrumental limitations [1], but also because of the tendency of their low-frequency range to be contaminated by facility-induced noise. Several solutions, including noise cancellation techniques, have been suggested to eliminate this noise [2], and shown to reduce the measured intensities substantially. In spite of those limitations, some general facts have been established for pressure fluctuations at the wall; for example, their root-mean-squared intensities, the general shape of their power spectra, and their space-time correlation characteristics. Reviews of the known experimental facts, mostly regarding wall pressures can be found in [3, 4, 5].

Numerical simulations have also contributed significantly to the understanding of pressure in turbulent flows, especially away from the wall [6, 7, 8]. For example, pressure has wall-attached spectra, and a well-developed logarithmic range of the fluctuation profile, and scales far from the wall with the friction velocity and with the flow thickness. As a consequence, when the fluctuations at the wall are scaled in inner variables, they increase logarithmically with the Reynolds number [7, 9]. Moreover, pressure fluctuations depend on the type of flow, and are stronger in boundary layers than in channels due to the intermittent character of the outer edge of the former [8, 10].

The computational equivalent of the acoustic contamination in experiments arises from the boundary conditions associated with the finite numerical domain. The contamination of pressure fluctuations, a common problem in simulations and experiments is partly responsible for why, even now, there are few published data on pressure, particularly away from the wall. The problem is well known, and there have been empirical recipes to minimize it, but, to the best of our knowledge, the root cause of the problem has remained unclear, and that is the focus of this paper. We will discuss how the pressure statistics are affected by the inflow conditions in direct numerical simulations (DNS) of zero-pressure-gradient spatially-developing turbulent boundary layers, using as example the problems found in a recent simulation from our group [11].

The numerical setup is described in Section 2, and the results for the velocity and uncorrected pressure

Table 1: Parameters of the turbulent boundary layer simulations. L_x, L_y and L_z are the box dimensions along the three axes. N_x, N_y, and N_z are the corresponding grid sizes, and the Δ values are the resolutions in wall units. The momentum thickness, θ, is measured at the middle of each box. The heights of the simulation boxes are given in terms of the boundary layer thickness δ_T at the transfer plane used to feed the inflow of BL6600, which is located at $L_x/\theta \approx 410$ of BLAUX.

Case	Re_θ	$(L_x, L_y, L_z)/\theta$	$\Delta x^+, \Delta y^+_{min}, \Delta z^+$	N_x, N_y, N_z	L_y/δ_T
BLAUX	1100-2970	$481 \times 47 \times 191$	$13 \times 0.32 \times 7.3$	$3585 \times 315 \times 2560$	4.20
BL6600	2780-6650	$547 \times 29 \times 84$	$7 \times 0.32 \times 4.1$	$15361 \times 535 \times 4096$	5.80

statistics are discussed in Section 3, followed by the proposed inflow correction procedure in Section 4, and by summary and conclusions.

2   The Numerical Simulation

The simulation is performed in a parallelepiped with a no-slip smooth wall, spanwise periodicity, and stream-wise non-periodic inflow and outflow, using the code in Ref. [12]. The streamwise, wall-normal and span-wise directions and velocity components are x, y, z and u, v, w, respectively, and the kinematic pressure p incorporates the constant fluid density. Capital letters refer to mean quantities, and primed ones to root-mean-squared fluctuation intensities. The + superscript denotes wall-scaled quantities, normalized with the x-dependent friction velocity u_τ and with the kinematic viscosity. The 99% boundary-layer thickness is δ.

The numerical code integrates the incompressible Navier-Stokes equations expressed in primitive variable form using a fractional step method together with a semi-implicit Runge-Kutta time scheme. The spatial discretization uses high-order compact finite differences in the non-periodic streamwise and wall-normal directions, and a Fourier expansion in the spatially periodic spanwise direction. The parallelization of the code is discussed in detail in [12, 11], including a full discussion of the numerical scheme and examples of applications to other problems.

To prescribe time dependent inflow conditions, we use the rescaling/recycling technique in Ref. [13]. In that paper, intended as a large-eddy simulation (LES), there are two distinct simulations. The first one is a DNS of an initial stretch of the boundary layer, one of whose downstream planes is rescaled and used to create its own inflow. The purpose of that auxiliary layer is to provide a natural turbulent flow in an intermediate plane, which is filtered and transferred to the inflow of the LES. A previous DNS from our group [12], of a turbulent boundary layer with a Reynolds number based on the momentum thickness $Re_\theta = 2100$, generated its inflow by recycling a single simulation, as in the auxiliary layer in Ref. [13]. A later attempt to extend it to the range $Re_\theta = 6500$ showed that the initial transition length required by the large scales of boundary layers to reach equilibrium is too long for a single simulation to be run economically [11], and we reverted to a two-simulation code in which the inflow of the main simulation, BL6600, is provided by an auxiliary boundary-layer simulation, BLAUX, running concurrently at lower Reynolds number and somewhat coarser resolution. Its purpose is to allow the larger scales to reach their asymptotic state before being used in the inflow of BL6600, and its computational cost is about 8% of the total. The resolution of the main simulation BL6600 is comparable to previous high-Reynolds number DNSes of channels [14] and boundary layers [12]. Table 1 summarizes the numerical parameters of both layers.

The mean pressure gradient is controlled by imposing at the top boundary an x-dependent suction velocity, constant in time, estimated from experimental correlations of the displacement thickness δ^* [15]. Continuity then implies that the instantaneous mass flux at each downstream section is determined by the inflow. As in [12], the recycling implementation of BLAUX only rescales the velocity fluctuations while fixing the inflow mean velocity to a prescribed empirical profile [15]. This ensures a constant inflow mass flux, although the code allows for minor adjustments to the outflow convective boundary condition, to enforce mass conservation [12]. For both layers, the resulting streamwise pressure gradient is $\delta^* U_\infty^+ \partial_x U_\infty^+ \approx 10^{-3}$.

To minimize the free-stream fluctuations, the height of the computational domain of BL6600 is chosen as 2.4 times the boundary-layer outflow thickness [12]. Using the same height for BLAUX would have increased the computational cost considerably with little physical gain, since its lower Reynolds number means that

most of the box height would be free stream. Computational load balancing finally suggested decreasing the height of BLaux by 25%. The mean velocity and fluctuations obtained from the transfer plane are interpolated to the finer grid of BL6600, and extended into its free stream as a uniform velocity.

In our implementation of the recycling method for BLaux we only rescale the velocity fluctuations while fixing the inflow mean velocity to a prescribed empirical [15], which we had also found useful in our previous boundary layer simulation [12], but the reasons why that was found useful were not analyzed in detail in that paper. That is discussed in the following section.

3 Results

BL6600 is one of the highest-Reynolds-number boundary layer simulations presently available, and will be discussed in detail in future papers. Here we only concern ourselves with the pressure fluctuations, and with the reasons why they did not initially agree with experiments.

Preliminary statistics of the velocity and vorticity were compiled over a time interval of $tu_\tau/\delta = 11.5$ eddy-turnovers, measured at the middle of the BL6600 box. Figure 1 presents the streamwise mean velocity and fluctuation intensities averaged over a window size of δ in the streamwise direction. Although the present simulation covers a wider range, statistics are presented at $Re_\theta = 5150$ ($Re_\tau \approx 1950$) to match the available boundary layer experimental data [16, 17] and turbulent channel data [14]. As shown here and in Ref. [11] velocity statistics agree very well with previous simulations and experiments.
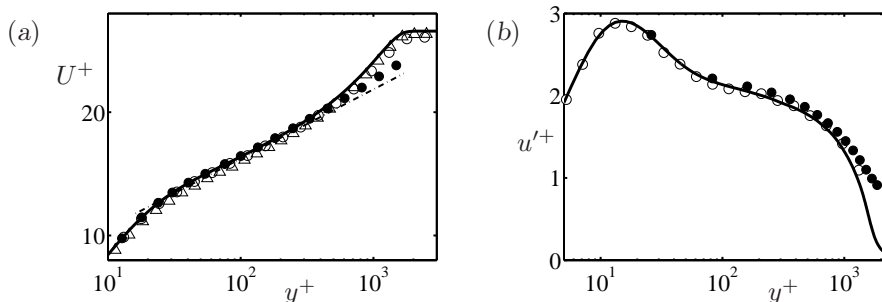

Figure 1: (a) Mean streamwise velocity. (b) Root-mean-squared streamwise velocity fluctuation. ——— , Present simulation at $Re_\theta = 5150$. ○, boundary layer experiments by de Graaff & Eaton (2000) at $Re_\theta = 5160$; △, Osterlund *et al.* (2000) at $Re_\theta = 5156$; and ●, numerical channel from Hoyas & Jimenez (2006) at $Re_\tau = 2000$, and $-\cdot-$, $\log(y^+)$ / $0.41 + 5$.

On the other hand, as depicted in Fig. 2, pressure fluctuation intensities for that first set of statistics do not agree with experiments (not included for visual clarity). After a sharp drop near the inflow, which can be traced to numerical effects and is not included in the figure, they remain relatively high, with a minimum around the middle of the box. The wall fluctuations, p'^{2+}, in Fig. 2(b) are approximately parabolic in x, and their well-known logarithmic Reynolds number dependence [7, 9] is lost. The pressure fluctuation profiles in Fig. 2(c) neither collapse far from the wall, nor do they vanish in the free stream. No such behaviour was found in BLaux.

The analysis of the pressure spectra showed that the extra intensity was confined to the largest flow scales, with streamwise wavelengths of the order of the computational box. For example, the pressure at the wall tracks that at the free stream (Fig. 3a) and the pressure fluctuations at the outflow are in antiphase with those at the inflow. The reason was traced to the variation of the inflow mass flux F of the main simulation. As noted earlier, its inflow is transferred from a plane of BLaux. The velocities are interpolated to the finer grid for BL6600, and extrapolated into the free stream by copying the last grid point to the taller box. It is that extension that changes the mass flux, because, although the flux through the transfer plane of the auxiliary box is kept constant by the constant inflow profile, the free-stream velocity varies slightly with time. If its variation is ΔU_∞, and the difference of the two box heights is ΔH, the flux changes by $\Delta U_\infty \Delta H$. In our simulation, that variation is less than 1%, but it is amplified into large pressure fluctuations by the large aspect ratio of the computational box.
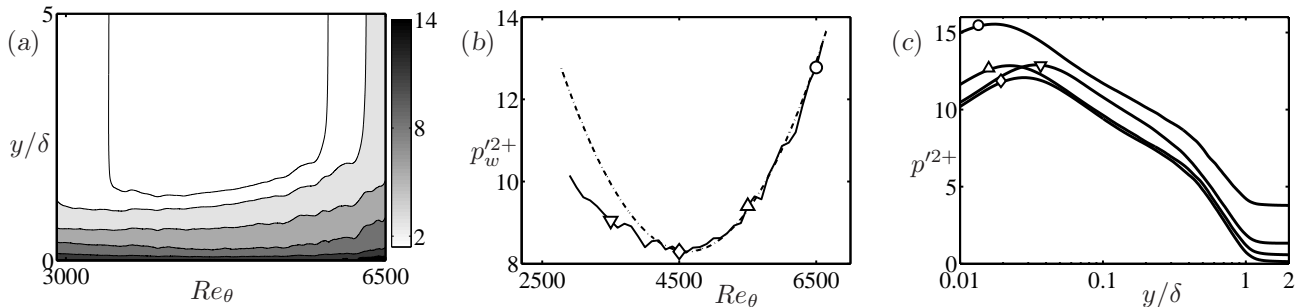
Figure 2: (a) Pressure fluctuation intensities, p'^{2+}. (b) At the wall. (c) Profiles of the pressure fluctuation intensities. $\triangledown$, $Re_\theta = 3500$; $\lozenge$, $Re_\theta = 4500$; $\triangle$, $Re_\theta = 5500$; $\circ$, $Re_\theta = 6500$.

Consider an inflow flux $F(t)$. The outflow boundary condition tracks it by adding an extra velocity at the last plane which is equivalent to a delta function in the velocity divergence. The pressure sub-step corrects that increment by creating a global linear pressure gradient, approximately independent of y. From the momentum equation,

$$\partial P/\partial x = -H^{-1} \int_0^H (\partial U/\partial t)\, \mathrm{d}y = -H^{-1}(dF/dt), \tag{1}$$

where H is the box height, which translates into a pressure difference,

$$\Delta P = P(0) - P(L_x) = (\,\mathrm{d}F/\,\mathrm{d}t)(L_x/H). \tag{2}$$

Figure 3(a) shows that this estimate agrees well with the data, and that the pressure difference is in phase with the time derivative of the flux. The correlation coefficient of ΔP and dF/dt is approximately 0.85, and the linear pressure distribution implied by Eq. (1) is consistent with the parabolic distribution in Fig. 2. Equation (2) reveals that the pressure due to a given flux variation is proportional to the aspect ratio L_x/H, which is approximately 20 in our case. A shorter test simulation with a similar computational setup and $L_x/H \approx 3$ showed a much weaker effect.

The flux variation in our case is small, but those in the original Lund's recycling [13], in which not only the fluctuations but the mean profile are rescaled to the inflow, can be much larger, because the flux is not preserved by rescaling. That may be the reason for some of the problems found in using that method, and, in retrospect, the reason why Ref. [12] found useful to fix the inflow mean velocity profile, rather than to rescale it. It is also probable that some of the large-scale pressure oscillations found in experiments [2] are related to small variations of the mass flux in the facility.

4   Mass-flow correction

Using a fixed inflow profile avoids the problem when a reasonable approximation is known from experiments [12], although it should be noted that even slightly incorrect profiles can modify the Reynolds stresses substantially [19], leading again too long inflow adaptation lengths. Another possibility is to base Lund's rescaling on the displacement thickness, instead of on the momentum thickness, which tends to fix the mass flux [20]. The solution adopted in our simulation was to apply to the instantaneous streamwise velocity profile of the transfer plane of BLAUX a correction factor,

$$U = (F_0/F_T)U_T(t), \tag{3}$$

where U_T is the velocity interpolated from BLAUX, F_T is its mass flux, and F_0 a reference flux chosen for the inflow of BL6600, for example, from a long-term average. Figures 3(b,c) present statistics compiled over 7.2 eddy-turnover times of a simulation thus corrected, and show that the extraneous pressure fluctuations have disappeared. The pressure fluctuations at the wall, represented in Fig. 3(b), increase logarithmically with the Reynolds number, in agreement with previous experimental [3] and numerical observations [7, 8]. The
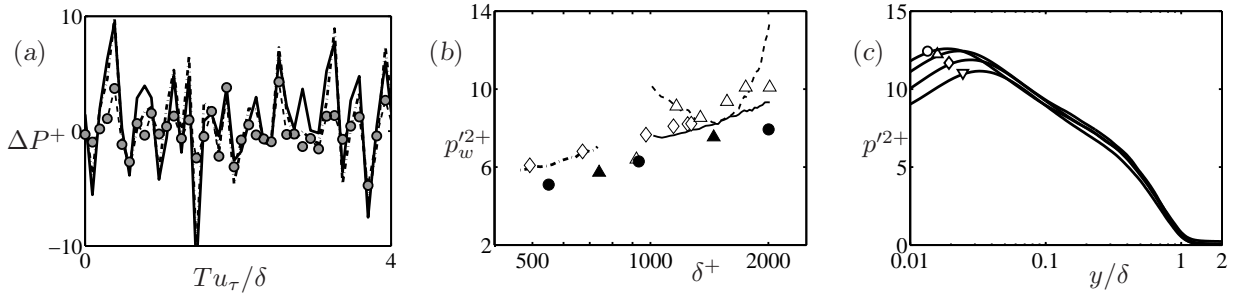
Figure 3: (a) Time evolution of the pressure difference, ΔP^+. ——, at the free-stream; —·—, at the wall; ——●——, Eq. (2). Wall units based on box middle section. (b) Pressure fluctuation intensities at the wall as a function of δ^+. Numerical boundary layers: ——, present, corrected; ——, present, uncorrected; —·—, Ref. [10]; $\diamond$, Ref. [18]. Experimental boundary layers: $\triangle$, Ref. [3]. Numerical channels: ●, Ref. [14]; ▲, Ref. [7]. (c) Profiles of the pressure fluctuation intensities after the flux correction. Symbols as in Fig. 2(c).

pressure profiles in Fig. 3(c) collapse well far from the wall, and vanish in the free stream. The correction factor, F_0/F_T, was always in the range $1 \pm 2 \times 10^{-4}$ in our simulation. Although not shown, the effect of this correction on the velocity statistics is less than the statistical uncertainty of the data, even in the contaminated simulation, since the pressure gradients induced by the mass flux variation are negligible compared with any of the other pressure gradients in the flow ($\Delta P^+/L_x^+ \approx 3 \times 10^{-5}$).

The acoustic oscillations in experiments are sometimes approximately compensated by subtracting the instantaneous free-stream pressure from the measured profiles [2, 1]. The same can be done here for each instantaneous field, because the large-scale pressure gradients at the wall and at the free-stream agree well (Fig. 3a), but cannot be used on the compiled fluctuation profiles. That would only be valid if the inner and outer fluctuations were statistically independent. While that is approximately true near the wall, it is not true near the edge of the layer.

A similar effect is familiar from simulations and experiments of internal flows, where channels and pipes are driven by a pressure gradient that is subtracted before fluctuations are defined. For example, turbulent channels have traditionally been simulated indistinctly by keeping either a constant mass flux, which implies a time-dependent pressure gradient, or by imposing a fixed pressure gradient. It was informally tested in the early channel DNSes that the statistics did not depend on the method. Channels in our group have always been run at constant flow rate by adjusting the pressure gradient dynamically, and to test once more that the variable driving pressure does not affect the statistics, we have performed two new channel simulations at $Re_\tau = 350$, one with constant mass flow and another with fixed pressure gradient. As expected, the two approaches yield the same velocity and pressure statistics, available from [21], and the variable pressure gradient induced by the mass flux variation is negligible compared with any of the other pressure gradients in the flow.

5 Summary and conclusions

In summary, we have shown that pressure statistics in computational turbulent boundary layers can be severely contaminated by minor variations of the mass-flux rate at the inflow, with an amplification factor proportional to the aspect ratio of the computational box. That effect constrains the use of the full recycling/rescaling method in Ref. [13], and requires that either the inflow mean profile be fixed, rather than rescaled, or that the rescaling be such that the mass flux is accurately constant. We have presented a DNS of a boundary layer at moderately high Reynolds number, in which the flux variation was introduced by extrapolating a feeder simulation to the taller free stream of the main box. Flow variations of less than 1% increased pressure fluctuations by about 30%, but they could be corrected by applying a dynamic rescaling factor to the mean inflow velocity to fix the mass-flux. Since the spatial scale of the extra pressure fluctuations is very large, their gradients are negligible compared with other gradients in the flow, and the velocity and vorticity statistics are unaffected. Even the pressure statistics can be approximately recovered by sub-

5

tracting the free-stream pressure from each instantaneous field, as in simulations of internal flows and in some experiments. We have argues that this effect is also responsible for some of the acoustic contamination in laboratory experiments.

References

[1] Y. Tsuji, J.H.M. Fransson, P.H. Alfredsson, and A.V. Johansson. Pressure statistics and their scaling in high-Reynolds-number turbulent boundary layers. *J. Fluid Mech.*, 585:1–40, 2007.

[2] G.C. Lauchle and M.A. Daniels. Wall-pressure fluctuations in turbulent pipe flow. *Phys Fluids*, 30(10):3019–3024, 1987.

[3] T.M. Farabee and M. Casarella. Spectral features of wall pressure fluctuations beneath turbulent boundary layers. *Phys. Fluids*, 3:2410–2419, 1991.

[4] W.W. Willmarth. Pressure fluctuations beneath turbulent boundary layers. *Annu. Rev. Fluid Mech.*, 7:13–38, 1975.

[5] M.K. Bull. Wall-pressure fluctuations beneath turbulent boundary layers: Some reflections on forty years of research. *J. Sound Vib.*, 190:299–315, 1996.

[6] J. Kim. On the structure of pressure fluctuations in simulated turbulent channel flow. *J. Fluid Mech.*, 205:421–451, 1989.

[7] Z.W. Hu, C.L. Morfey, and N.D. Sandham. Wall pressure and shear stress spectra from direct simulations of channel flow. *AIAA J.*, 44(7):1541–1549, 2006.

[8] J. Jiménez and S. Hoyas. Turbulent fluctuations above the buffer layer of wall-bounded flows. *J. Fluid Mech.*, 611:215–236, 2008.

[9] J. Jiménez and R.D. Moser. What are we learning from simulating wall turbulence. *Phil. Trans. R. Soc. A*, 365:715–732, 2007.

[10] J. Jiménez, S. Hoyas, M.P. Simens, and Y. Mizuno. Turbulent boundary layers and channels at moderate Reynolds numbers. *J. Fluid Mech*, 657:335–360, 2010.

[11] J. Sillero, J. Jiménez, R.D. Moser, and N.P. Malaya. Direct simulation of a zero-pressure-gradient turbulent boundary layer up to $Re_\theta = 6650$. *J. Phys: Conf. Ser.*, 318(022023), 2011.

[12] M.P. Simens, J. Jiménez, S. Hoyas, and Y. Mizuno. A high-resolution code for turbulent boundary layers. *J. Comput. Phys.*, 228:4218–4231, 2009.

[13] T.S. Lund, X. Wu, and K.D. Squires. Generation of turbulent inflow data for spatially-developing boundary layer simulations. *J. Comput. Phys.*, 140:233–258, 1998.

[14] S. Hoyas and J. Jiménez. Scaling of the velocity fluctuations in turbulent channels up to $Re_\tau = 2003$. *Phys. Fluids*, 18:011702, 2006.

[15] H.M. Nagib, K.A. Chauhan, and P.A. Monkewitz. Approach to an asymptotic state for zero pressure gradient turbulent boundary layers. *Phil. Trans. R. Soc. A*, 2007.

[16] D.B. De Graaf and J.K. Eaton. Reynolds number scaling of the flat-plate turbulent boundary layer. *J. Fluid Mech.*, 422:319–346, 2000.

[17] J.M. Osterlund, A.V. Johansson, H.M. Nagib, and M. Hites. A note on the overlap region in turbulent boundary layers. *Phys. Fluids*, 12:1–4, 2000.

[18] P. Schlatter and R. Örlü. Assessment of direct numerical simulation data of turbulent boundary layers. *J. Fluid Mech.*, 659:116–126, 2010.

[19] F. Tuerke and J. Jiménez. Simulations of turbulent channels with prescribed mean velocity profiles. *J. Fluid Mech., submitted*, 2011.

[20] J.W. Jewkes, Y.M. Chung, and P.W. Carpenter. Modification to a turbulent inflow generation method for boundary-layer flows. *AIAA J.*, 49(1):247–250, 2011.

[21] http://torroja.dmt.upm.es/ftp/channels/.